Molecular characterization of binding loop E in the nematode cys-loop GABA receptor

Ariel Kwaka, Mohammad Hassan Khatami, Joshua Foster, Everett Cochrane, Sarah A Habibi,

Hendrick W de Haan and Sean G. Forrester

Faculty of Science, University of Ontario Institute of Technology (UOIT)

Running Title page

Nematode GABA receptor binding loop

Author for correspondence: Sean Forrester

University of Ontario Institute of Technology, 2000 Simcoe Street North, Oshawa ON L1H 7K4,

Canada 1-905-721-8668; FAX 905-721-3304, sean.forrester@uoit.ca

Number of text pages: 34

Number of tables: 2

Number of Figures: 8

Number of references: 36

Number of words in abstract: 225

Number of words in introduction: 741

Number of words in discussion: 1260

Abbreviations used in this study: UNC, uncoordinated; SCAM, substituted cysteine accessibility method; MTSET, (2-(trimethylammonium)ethyl methanethiosulfonate); DAVA, 5-Aminovaleric acid; MD, molecular dynamics

Abstract

Nematodes exhibit a vast array of cys-loop ligand-gated ion channels with unique pharmacological characteristics. However, many of the structural components that govern the binding of various ligands are unknown. The nematode cys-loop GABA receptor UNC-49 is an important receptor found at neuromuscular junctions, and plays an important role in the sinusoidal movement of worms. The unique pharmacology of this receptor suggests that there are structural differences in the agonist binding site when compared to mammalian receptors. In this study, we examined each amino acid in one of the main agonist binding loops (loop E) via the substituted cysteine accessibility method (SCAM) and analysed the interaction of various residues by molecular dynamic simulations. It was found that of the 18 loop E mutants analyzed, H142C, R147C and S157C had significant changes in GABA EC_{50} and were accessible to modification by a methanethiosulfonate reagent (MTSET) resulting in a change in I_{GABA}. In addition, the residue H142, which is unique to nematode UNC-49 GABA receptors, appears to play a negative role in GABA sensitivity as its mutation to cysteine increased sensitivity to GABA and caused the UNC-49 receptor partial agonist 5-aminovaleric acid (DAVA) to behave as a full agonist. Overall, this study has revealed potential differences in the agonist binding pocket between nematode UNC-49 and mammalian GABA receptors that could be exploited in the design of novel anthelmintics.

Introduction

Nematodes such as the model free-living nematode *Caenorhabditis elegans,* and parasitic nematodes such as *Haemonchus contortus,* contain a vast array of cys-loop ligand-gated chloride channels that respond to a variety of neurotransmitters including serotonin, tyramine, dopamine, GABA and glutamate (Bartos et al., 2009; Jones and Sattelle, 2008; Laing et al., 2013). In addition, nematodes exhibit a unique class of acetylcholine-gated chloride channels (Putrenko et al., 2005) and GABA-gated cation channels (Beg and Jorgensen, 2003). However, like vertebrates, nematodes also exhibit anion selective receptors for GABA. The nematode cys-loop GABA receptor that is the most characterized pharmacologically and functionally is the UNC-49 receptor (Bamber et al., 1999; Siddiqui et al., 2010). This receptor is expressed at the neuromuscular junctions of nematodes, and contributes to the worm's sinusoidal movement (Bamber et al., 2005). With regard to amino acid sequence, the UNC-49 receptor does not appear to be analogous to any mammalian GABA receptor, and appears to exhibit a unique pharmacology. One significant pharmacological difference is the low sensitivity of the classical GABA receptor antagonist bicuculline (Bamber et al., 2003) which is a characteristic shared among invertebrate GABA receptors (Hosie et al., 1997). Differences have also been observed between the agonist profile of the UNC-49 receptor from *H. contortus* (Hco-UNC-49) and the mammalian receptors. Most notable is the insensitivity of the nematode receptor to sulphonated compounds such as taurine and P4S, which have been shown to exhibit efficacy at the mammalian GABA$_A$ receptor (Kusama et al., 1993; Woodward et al., 1993; del Olmo et al., 2000; Kaji et al., 2015). The unique pharmacology of nematode cys-loop GABA receptors suggest that there are structural differences in the agonist binding pocket. However, compared to their mammalian counterparts, there is little known about the structural elements that govern agonist binding to nematode GABA receptors.

The binding site of cys-loop receptors is made up of six discontinuous loops, designated

by the letters A-F. The number of loops and their general position appear conserved across phyla

(Brejc et al., 2001; Hibbs & Gouaux, 2011). Loops A-C are found within the primary subunit,

while loops D-F are in the adjacent subunit. The role of various binding loop residues in the

function of mammalian GABA receptors have been examined through site-directed mutagenesis

and SCAM. SCAM analysis involves changing predicted binding site residues to cysteines via

site-directed mutagenesis. If the introduced cysteine is modified by a reducing agent such as

MTSET (see Figure 1), GABA binding should be reduced if that cysteine resides is in the binding

pocket. Binding pocket residues are confirmed through the use of agonists and antagonists which

would slow the rate of modification of the introduced cysteines by reducing agents (Kloda and

Czajkowski, 2007). However, it is important to note that modification of cysteines by molecules

such as MTSET could have more complex effects on receptor activation and thus results should

be interpreted with caution.

The detailed knowledge that we now have on the structure of the GABA binding pocket in

mammalian GABA receptors has provided an opportunity for comparative analyses on GABA

receptors from more primitive organisms such as nematodes. Several residues in loops A-D have

previously been examined in the Hco-UNC-49 receptor through site-directed mutagenesis which

revealed functional similarity when compared to mammalian GABA receptors (Accardi and

Forrester 2011). Binding loop E, on the other hand, is made up of 18 residues and the residues that

play key roles in ligand binding have been mapped in both the GABA$_A$ α1 and the GABAc ρ1

subunits via SCAM analysis (Kloda and Czajkowski, 2007; Sedelnikova et al., 2005). We aligned

loop E from these two GABA receptor classes with the Hco-UNC-49 receptor, revealing 12

positions that are not completely conserved (Figure 2). Interestingly, residues such as H142 and

F145 appear to be conserved among nematode UNC-49-like receptors. We wondered whether unique residues present in loop E of nematode GABA receptors have any functional significance when compared to published reports on mammalian receptors and could possibly explain some of the pharmacological characteristics observed. Here, we have conducted an examination of each residue in loop E from the *H. contortus* UNC-49 receptor using site-directed mutagenesis and SCAM; two methods that have been used to characterise the mammalian GABA binding site and should allow some insight into differences between mammalian and nematode GABA receptors. Of the residues examined experimentally and via molecular dynamic simulations, some appeared to have similarity in function with mammalian receptors, whereas others could have some functional differences.

Methods

Site-Directed Mutagenesis – Primer Design

Amino acid alignments of Hco-UNC-49B and other GABA receptor subunits in the ligand-gated chloride channel (LGCC) family, were used to determine the location of loop E within the *H. contortus* sequence (Figure 2). Primers were designed using Stratagene's web-based QuikChange® Primer Design program (www.stratagene.com/sdmdesigner/default.aspx) to create 18 *Hco-unc-49b* (Genbank Accession # EU939734.1) mutants (H142C, N143C, S144C, F145C, L146C, R147C, I148C, D149C, S150C, D151C, G152C, T153C, V154C, Y155C, T156C, S157C, Q158C, and R159C). Each pair of mutagenic primers were designed to change each amino acid residue within loop E into cysteine residues, by way of nucleotide introduction, resulting in singly mutated cysteine mutants.

Site-Directed Mutagenesis of *Hco-unc-49b*

Previous work in our lab found that the binding site for GABA in the Hco-UNC-49BC channel was at the interface of two adjacent UNC-49B subunits. However the exact stoichiometry of the heteromeric channel is unknown (Accardi and Forrester, 2011). The template used in the site-directed mutagenesis of *Hco-unc-49b* was previously sub-cloned into a pT7Ts transcription vector, in which *Xenopus laevis* β-globin untranslated DNA was incorporated into the 5' and 3' ends of the Hco-UNC-49B subunit cDNA (Siddiqui *et al.,* 2010).

A naturally occurring cysteine residue located at position 224 of the template amino acid sequence was removed through site-directed mutagenesis to prevent interference with results obtained from the introduced cysteine residues. With no alteration in function (Figure 3; Table 1), the cysteine-

less mutant (C224A) was used as template, and a baseline from which all data obtained could be compared to throughout.

All site-directed mutagenesis performed was conducted using the QuikChange ® Site-Directed Mutagenesis Kit (Stratagene, La Jolla, CA, USA) according to the manufacturer's instructions. Confirmation that the correct mutation was present was verified using DNA sequencing (Genome Quebec).

cRNA Preparation – *In Vitro* Transcription

Plasmid constructs containing either the mutated *Hco-unc-49b* and wild-type (WT) *Hco-unc-49c* (Genbank Accession # EU049602.1) were linearized and used as template (0.4-1 µg) to create capped *Hco-unc-49* copy RNA (cRNA). The cRNA was made using the mMessage mMachine *in vitro* transcription reaction and the T7 RNA polymerase provided within the transcription kit (Ambion, Austin, TX, USA). cRNA was precipitated using lithium chloride, and brought to a concentration of 0.5 ng/L upon re-suspension in nuclease free water. Each *in vitro* transcription reaction yielded approximately 10-25 µg of cRNA.

Expression of Hco-UNC-49BC in *Xenopus laevis* Oocytes

Oocytes were obtained surgically from female *X. laevis* (Nasco, Fort Atkinson, WI, USA) which were housed in temperature controlled rooms at UOIT and according to the methodology outlined in Abdelmassih et al., 2018 and adhering to the UOIT Animal Care Committee and the Canadian Council of Animal Care guidelines. The frogs were anaesthetized with 0.15% 3-aminobenzoic acid ethyl ester methane sulphonate salt (MS-222; Sigma-Aldrich, Oakville, ON, CA). Lobes of the ovary were extracted, split into smaller pieces of 10-20 oocytes, and defolliculated in a treatment

of 2 mg/mL collagenase-II (Sigma-Aldrich) and OR2 solution (82 mM NaCl, 2m M KCl, 1m M MgCl$_2$, 5 mM HEPES pH 7.5) for two hours with gentle rocking at room temperature. After defolliculation, oocytes were stored at 20ºC in ND96 buffer (96 mM NaCl, 2 mM KCl, 1.8 mM CaCl$_2$, 1 mM MgCl$_2$, 5 mM HEPES pH 7.5) supplemented with 100 µg/mL gentamycin and 0.275 µg/mL pyruvic acid (Sigma-Aldrich). Supplemented ND96 solutions were replaced twice every 24-hour period.

Cytoplasmic injections of cRNA were carried out on stage V and VI oocytes using a Drummond Nanoject II (Drummond Scientific Company, Broomhall, PA, USA) assisted by micromanipulators (World Precision Instruments, Inc., Sarasota, FL, USA). Each oocyte was injected with 50 nL of a mixture of mutated *Hco-unc-49b* and WT *Hco-unc-49c* (equal amounts of 0.5 ng/nL cRNA of each). Electrophysiological recordings were taken after receptor expression, approximately 2-5 days after cRNA injection.

Compounds tested and their preparation

MTSET (2-(trimethylammonium) ethyl methanethiosulfonate) was obtained from Toronto Research Chemicals (Toronto, ON, CA). GABA, DAVA and pregnenolone sulfate were obtained from Sigma-Aldrich, Oakville, ON, CA. All compounds were initially dissolved in ND96 expect for PS which was dissolved in DMSO for the preparation of a stock solution. Compounds were diluted in ND96 as working solutions. Structures of compounds are found in Figure 1.

Two-Electrode Voltage Clamp (TEVC) Electrophysiology

Using an Axoclamp900A voltage clamp (Molecular Devices, Sunnyvale, CA, USA), TEVC electrophysiology was used to observe and record channel activity of the Hco-UNC-49B/C channel. Glass electrodes were pulled from borosilicate capillaries using a P-97 Flaming/Brown

micropipette puller (Sutter Instruments Company, Novato, CA, USA), and filled with 3M KCl (1-5 MΩ resistance). Each of the two electrodes were connected to Axon Instrument Headstages (Molecular Devices) using Ag|AgCl wires. Oocytes were held at a membrane voltage at -60mV throughout the experiment. Compounds were perfused over the oocytes (at 8 mL/min) through a gravitational flow system into an RC-1Z perfusion chamber (Warner Instruments Inc, Holliston, MA, USA). ND96 buffer was used to dilute the various compounds, in addition to being used as a wash solution in between drug applications. Recordings and associated data were obtained using Axon Instruments Digidata 1440, Clampex 10.2, and analyzed via Clampfit 10.2 (Molecular Devices).

EC_{50}s were determined for each mutant by perfusing increasing concentrations of GABA (or other agonists) and recording the current observed which included the concentration of agonist that produced maximal current.

For experiments using the negative allosteric modulator (NAM) of GABA receptors, pregnenolone sulfate (PS), oocytes expressing mutant or wildtype Hco-UNC-49BC receptors were first exposed to EC_{50} concentrations of GABA to ensure channel functionality. Oocytes were then exposed to a co-application of an increasing range (5µM to 500µM) of PS concentrations mixed with the corresponding EC_{50} GABA concentration. Changes in current were recorded and inhibitory dose response curves were generated to determine the IC_{50} value for the mutant being tested.

Substituted Cysteine Accessibility Method (SCAM)

SCAM was used to characterize all Hco-UNC-49B mutants as well as the cysteine-less mutant (C224A) using the reducing agent MTSET. During testing, an oocyte was washed and hit with EC_{20-50} concentrations of GABA in 5-minute intervals until response stabilized within 10%. Once stabilized, MTSET (1mM for 1 min) was perfused over the oocyte, followed by 5 min of wash

with ND96 solution. The EC$_{20\text{-}50}$ concentrations of GABA for the mutant being tested was re-applied, and currents were recorded (Sedelnikova et al., 2005, and Kloda and Czajkowski, 2007).

Statistical Analysis

Dose-response curves were generated by Prism 5.0 (Graphpad Software, San Diego, CA, USA) using the following equation in the set-up log (agonist) vs. normalized response-variable slope:

$$Imax = \frac{1}{1 + \left(\frac{EC50}{[D]}\right)^h}$$

Where I_{max} is the maximal response, [D] is the concentration of agonist, EC$_{50}$ is the concentration of agonist that is required to produce half-maximal current, and *h* is the Hill coefficient. Responses used to produce dose-response curves were normalized as a percentage of the maximal current produced by the oocytes individual maximal response to GABA.

The effect of MTSET modification was calculated using the following formula:

$$\left(\frac{I_{GABA-post}}{I_{GABA-pre}}\right) - 1$$

Where $I_{GABA\text{-}post}$ is the current produced from GABA activation of the receptor after the application of MTSET, and $I_{GABA\text{-}pre}$ is the current produced from GABA activation before MTSET was applied (Kloda and Czajkowski, 2007).

EC$_{50}$ values, *h* values, and standard error (S.E.) were determined using Prism 5.0 from a minimum of five oocytes from two different *X. laevis*. Statistical significance was derived from student t-tests utilizing the Bonferroni correction or a one-way ANOVA with the Dunnet's multiple comparison test. *P*<0.001 was used to determine the level of significance in all analyses.

11

Homology modelling

The *C. elegans* glutamate-gated chloride channel crystal structure (PDB 3RIF; Hibbs & Gouaux, 2011) was used as a template in MODELLER 9.14 (Sali & Blundell, 1993) for the generation of a Hco-UNC-49B extracellular domain homodimer (Data Supplement PDB File). The most energetically favorable models were determined based on their DOPE score and PROCHECK Ramachandran plot analysis as described in Kaji et al., 2015.

Computational agonist docking

The energetically reduced zwitterion form of GABA was obtained from the Zinc database, http://zinc.docking.org/ (Irwin et al., 2012). The GABA molecule was prepared for docking using AutoDock Tools (Morris et al., 2009) and was docked using AutoDock Vina (Trott and Olson, 2010). The center of the 30x30x30 Å search box located in the aromatic box of the agonist binding site was used for agonist docking. A maximum of 50 binding models all within a range of 5 kcal mol^{-1} from the best scoring pose was generated (Kaji et al., 2015).

MD simulations

The homology model of the protein generated above, containing the docked GABA molecule in the binding area, was used as the initial structure for the molecular dynamics (MD) simulations. The GROMACS 2016.4 software package (Abraham et al., 2017), employing the CHARMM36 force field (Best et al., 2012), was used to run the simulations. The CHARMM General Force Field (CGenFF) program, which is an automated method to provide parameters and charges by analogy (Vanommeslaeghe et al., 2010; Yu et al., 2012; Vanommeslaeghe and MacKerell 2012; Vanommeslaeghe et al., 2012; CGenFF interface https://cgenff.paramchem.org) was used to acquire the CHARMM force field parameters for the GABA molecule. The simulation box was

12

solvated with ~21000 tip3p water molecules, along with Cl^- counter ions to neutralize the total charge of the system. To carry out the MD simulation, after a brief energy minimization, a 2 ns equilibration simulation was performed under the NVT conditions at 300 K and a time step of 2 fs. The positions of the protein and the ligand were restrained to prevent any structural changes during the equilibration process. In the production run, under the NPT conditions, the system was kept at 300 K and 1 atm with a time step of 2 fs for 500 ns. The Parrinello-Rahman isotropic pressure coupling (with $\tau p = 5$ ps and compressibility 4.5×10^{-5} bar $^{-1}$) and the Nose-Hoover thermostat (with a time constant of 0.1 ps) were employed for these production runs. Long-range electrostatics were calculated with the particle mesh Ewald method. The trajectory was printed every 10 ps.

The gromacs utilities, such as gmx, mpi mindist, gmx_mpi gyrate and gmx_mpi rms, as well as the H-bond calculator plugin of visual molecular dynamics (vmd) (Humphrey et al., 1996; http://www.ks.uiuc.edu/Research/vmd/) were used to calculate the results. The default values for distance (d) and angle (θ) ($d<3.0$Å and $\theta<20°$) are used to determine the H-bonds. Ionic bonds between oppositely charged residues were determined at $d<3.0$Å.

Results

Characterization of Loop E Cysteine Mutants in Hco-UNC-49BC

The importance of loop E amino acid residues in the Hco-UNC49 receptor was first assessed by determining the impact of each cysteine mutation on GABA-activation of the channel. Each loop E mutant was exposed to increasing concentrations of GABA to determine EC_{50} values. Upon recording, good expressions of all receptors with mutated subunits were observed, all receptors were functional, and clean tracings were obtained (Figure 3A). The cysteine-less mutant, C224A, was an appropriate control for this study as the GABA EC_{50} (33 µM) was similar to wildtype (40 µM; Siddiqui et al 2010) and this mutant was not sensitive to MTSET treatment.

Of the 18 mutants tested, 12 showed a substantial shift in GABA EC_{50} compared to the C224A cysteine-less mutant from which they were derived (representative dose-response curves are seen in Figure 3B). Of the mutants that displayed a different EC_{50} from C224A (33µM ± 2), H142C showed an increase in GABA sensitivity (2.7µM ± 0.2). The remaining 11 mutants (N143C, S144C, F145C, L146C, R147C, S150C, T153C, V154C, Y155C, T156C, S157C, and R159C) had a decrease in GABA sensitivity, with S157C and R159C showing the greatest decrease (3683.50µM ± 413.66 and 3102.33µM ± 130.43 respectively). Finally, 6 of the cysteine mutants, I148C, D149C, S150C, D151C, G152C and Q158C, showed minimal change in GABA EC_{50}. EC_{50} values that were significantly different from C224A ($P>0.001$) are shown in Table 1.

14

Determination of Cysteine Accessibility

Substituted cysteine accessibility method (SCAM) was performed on all loop E Hco-UNC-49B mutants to determine: which were accessible to MTSET modification, and the impact of modification on channel function. Overall, it was found that most of the cysteine mutants were either not influenced or positively influenced by MTSET treatment. Specifically, out of the 18 mutants tested, only H142C, R147C, and S157C were significantly ($P<0.001$) impacted by MTSET modification (Figure 4). Furthermore, only S157C had a decrease in % change in I_{GABA} (-49.8 ± 7.8 %). Conversely, H142C and R147C all showed an increase in % change in I_{GABA} (88 ± 4 and 52.5 ± 17 %, respectively).

Pharmacological Characterization of H142C Mutant

Upon discovering significant hypersensitivity to GABA in H142C two other compounds were investigated, 5-aminovaleric acid (DAVA) and pregnenolone sulfate (PS). Dose-response curves were created for both compounds (Figure 5A and 5C) with respect to the H142C mutant as well as the cysteine-less C224A baseline mutant. In addition, DAVA behaved as a partial agonist at the C224A receptor (I_{max} 21.2% ± 2.7), but as a full agonist at the H142C receptor (I_{max} 86.5% ± 2.8; Table 2). On the other hand, no significant difference was observed in the IC_{50} of PS between C224A and H142C receptors (Figure 5, Table 2). For the C224A receptor, the IC_{50} for PS was 47 μM compared to 70 μM for H142C.

15

MD Simulations

As a further analysis of loop E residues we conducted molecular simulations. To ensure that the simulations provided a meaningful analysis of the role of loop E residues and their possible impact on GABA binding we first examined the interaction of GABA with well-studied residues within the binding pocket. During the course of the simulation, the GABA molecule remained inside the initial binding pocket and interacted with key side chains previously implicated as essential for GABA binding in both mammalian (Newell et al., 2014) and the UNC-49 receptor (Accardi and Forrester 2011; Kaji et al., 2015) (Figure 6A). For example the positive amino group of GABA forms ionic bonds with carboxylate of E185 (loop B) 94% of the time. Likewise the carboxylate group of GABA forms ionic bonds with R87 (loop D) 99% of the time and S236 (Loop C) forms hydrogen bonds with GABA 35% of the time. These values were similar to MD simulations of the *Drosophila* RDL receptor (Ashby et al., 2012).

With respect to loop E residues, molecular simulations revealed only two residues forming hydrogen bonding with GABA. GABA most frequently formed H-bonds with S157 (74.25% of the time) and TYR155 (53.36% of the time) (Figure 6A and D).

ARG147 did not interact with the GABA molecule, except for the first few ns of the simulation (Figure 6B and 7A). Alternately, the R147 side chain mainly associated with the D149 side chain (Figure 7A) via and ionic bond (35% during the course of the simulation). However, the most recurrent interaction between the two residues was a H-bond between the backbone of R147 and Y155 as part of the anti-parallel β-sheet secondary structure of loop E (~81% as an acceptor and ~19% as a donor) (Figures 6B and 7B).

Electrostatic interactions between H142 and S144 were also observed. However, the interaction was variable and only 0.39% of the time was the interaction hydrogen bonding. The distance between these two groups fluctuated between ~1 nm (not interacting) and ~0.4 nm (interacting) (Figures 6C and 8). For the last 200ns of the simulation, the separation distance became more dynamic. Further investigation indicated that there was a small structural change in the structure of loop E at t ~300 ns, where the S144 and F145 (at the beginning of the loop) lose their β-structure (Supplemental Figure 1). However, this change did not have any major impact on the results calculated in the system (Supplemental Figure 2 and Supplemental Table 1).

Discussion

A comparative analysis of residues between mammalian and invertebrate GABA receptors can provide some valuable information on ligand-binding sites and receptor function. Indeed, a comparative mutagenesis approach was key to identifying the neurosteroid binding site in cys-loop GABA receptors (Hosie et al., 2006). This study describes the characterization of the eighteen residues found in binding loop E of the Hco-UNC-49 receptor. In this investigation we determined which residues, when mutated to cysteine, impacted the sensitivity of the Hco-UNC-49 receptor to GABA and other agonists. Moreover, exposure of the introduced cysteines to the reducing agent MTSET revealed which residues were accessible to MTSET modification (e.g. in an aqueous environment) and impacted GABA sensitivity. However, interpretation of SCAM results should be done with caution as molecules such as MTSET have been shown to have more complex effects such as acting as tethered partial agonists (Wang et al 2010). Alternatively the enhancement in IGABA might be caused by MTSET acting as a positive allosteric modulator.

This study revealed some loop E residues within Hco-UNC-49 that may exhibit similar properties as those found in human receptors, but also revealed several with possible distinct functions in the nematode receptor. Overall, it appears to that loop E of the Hco-UNC-49 receptor is more tolerant to cysteine mutagenesis than the $GABA_A$ receptor (Kloda and Czajkowski, 2007). Another distinction in the overall results of this study was that only one of the mutations (S157C) resulted in a decrease in I_{GABA} when modified by MTSET while others exhibited either no change or an increase in current. Studies on the human $GABA_C$ (which also used MTSET) receptor appeared to show the opposite trend (Sedelnikova et al., 2005). The results presented here may indicate an overall difference in the structure of loop E and the role it may play in nematode cys-loop GABA receptors when compared to their mammalian counterparts.

In this study six mutants (I148C, D149C, S150C, D151C, G152C and Q158C) did not impact the functionality of the receptor, exhibiting EC_{50} values close to those obtained from C224A (the cysteine-less mutant displaying WT function). According to our model (Figure 2), I148-G152 are at the top of loop E and therefore positioned ~13-17 Å away from GABA. Interestingly, the UNC-49 G152 residue, which is conserved among all GABA receptors, appears to be much more tolerant to a change to cysteine (1.7 fold-decrease) compared to mammalian receptors where this change resulted in either a 42-fold reduction in GABA sensitivity or non-functional receptors (Kloda and Czajkowski, 2007; Sedelnikova et al., 2005).

R147 appears to be conserved across many phyla (Figure 2). We found a small 2.7-fold change in EC_{50} when this arginine was mutated to a cysteine, and when MTSET was applied, there was a significant increase in GABA current. These results are very different from what was found for the $GABA_A$ α1 and the $GABA_C$ ρ1 receptors. When this arginine residue was mutated to a cysteine in the $GABA_A$ α1 subunit, there was a 260 fold decrease in EC_{50} compared to that of the wild-type (Kloda and Czajkowski, 2007), and the same mutation in GABAc ρ1 resulted in a receptor that was expressed too low for further analysis (Sedelnikova et al., 2005). However, in both receptors it was determined that this arginine does not directly interact with GABA. Homology modeling of the Hco-UNC-49 receptor suggests that R147 faces the binding pocket, but does not interact with GABA based on our MD simulations. However, the positive charge of MTSET (when bound to the introduced cysteine) may stabilize the negative carboxyl group of GABA, which may explain the increase in GABA current we observed after application. In the insect RDL receptor, mutations at this position (ie R166) with either an A or G produced non-functional channels. However, it was suggested that this residue was not likely to be essential for GABA binding (Ashby et al., 2012). It is possible that R147 has a different role in nematode

19

UNC-49 receptors compared to mammalian and possibly even *Drosophila* receptors. We found evidence for a molecular interaction between the side chains of R147 and D149 (Figure 7A). In the GABA$_A$ α1 and the GABA$_C$ ρ1 receptors the residues in the analogous positions as D149 are non-ionic polar residues (Figure 2). Therefore, the potential interactions between R147 and other residues may provide some unique features of the nematode GABA receptor.

H142C produced a hypersensitive channel. Treatment with MTSET revealed that the introduced cysteine was accessible for modification, and the resulting modification increased the GABA current. Our MD simulations suggests that H142 does not face the binding pocket, so it may impact the binding site in other ways. Indeed, the mutation H142C not only had a positive effect on GABA, but also effected the Hco-UNC-49 receptor partial agonist DAVA, converting it to a full agonist. This mutation however, had minimal effect on the sensitivity of the neurosteroid PS, a negative allosteric modulator shown to bind at a site away from the agonist binding site (Wardell et al., 2006). Since histidine is an amino acid with a positively charged bulky side group, it is possible that its removal results in structural changes which may positively impact both GABA and DAVA binding. One possibility is that H142 has some electrostatic interaction with S144 (Figure 6C and 8) and the H142C change alters this interaction which in turn alters the binding site. It is interesting that H142 appears to be conserved within the nematode phyla and is also present in the unique nematode cation GABA receptor EXP-1 (Beg and Jorgensen, 2003). The exact role of this residue in nematode receptors is unknown, but it could be involved in the unique pharmacology of nematode UNC-49-like GABA receptors.

One residue that may have similar functions across phyla is S157. Mutation of this position to cysteine produces a receptor that was 113-fold less sensitive to GABA, and when modified by MTSET, the GABA current is reduced. The analogous residues in the human GABA receptor is

T129 in the GABA$_A$ and the S168 in GABA$_C$ receptor. In both cases these residues were confirmed to lie within the binding pocket (Sedelnikova et al., 2005; Kloda & Czajkowski, 2007) where they form a H-bond with GABA. The molecular simulations also revealed high occurrences of H-bonds between S157 and GABA. In the insect RDL receptor it appears that a serine at this position is also essential where it makes a H-bond with the carboxyl group of GABA (Ashby et al., 2012). However, in the Hco-UNC-49 receptor, MD simulations also detected less frequent H-bonding between Y155 and GABA. The equivalent residue in mammalian receptors and several other GABA receptors is a non-polar leucine. We anticipate, that in the Hco-UNC-49 receptor, Y155 may play a minor role in GABA binding. However, whether it contributes to some unique functions of the nematode UNC-49 receptor will be focus of further study.

Conclusion

This was the first study that conducted a comprehensive analysis of a single binding loop from an invertebrate GABA receptor. It was found that of the loop E mutants analyzed H142C, R147C and S157C had significant changes in EC$_{50}$ and were accessible to modification by MTSET which affected GABA sensitivity. Furthermore, as a result of this study, H142 was identified as a residue that may have an important role in the sensitivity and selectively of the UNC-49 receptor. While more work is required to fully characterize the structure of the Hco-UNC-49 binding pocket, the work from this study suggests that there are structural differences when compared to mammalian receptors. This further highlights the potential of Hco-UNC-49 as a future drug target.

Acknowledgements

Author contributions:

Participated in research design: Kwaka, Forrester, de Haan

Conducted experiments: Kwaka, Foster, Cochrane, Habibi, Khatami

Contributed new reagents or analytic tools: Forrester, de Haan

Performed data analysis: Kwaka, Khatami

Wrote or contributed to the writing of the manuscript: Kwaka, Khatami, Forrester

Footnote:

References

Abdelmassih, SA, Cochrane, E & Forrester, SG (2018) Evaluating the longevity of surgically extracted *Xenopus laevis* oocytes for the study of nematode ligand-gated ion channels. *Invert Neuro* 18: 1.

Abraham, MJ, van der Spoel D, Lindahl E, Hess B, and the GROMACS development team (2017) *GROMACS User Manual version 2016.4*, www.gromacs.org

Accardi MV, Forrester SG (2011) The *Haemonchus contortus* UNC-49B subunit possesses the residues required for GABA sensitivity in homomeric and heteromeric channels. *Mol Biochem Parasitol* 178(1-2):15-22

Ashby, J. A., McGonigle, I. V., Price, K. L., Cohen, N., Comitani, F., Dougherty, D. A., Molteni, C., Lummis, S. C. (2012). GABA binding to an insect GABA receptor: a molecular dynamics and mutagenesis study. *Biophy J* 103(10), 2071-2081.

Bamber, BA, Beg, AA, Twyman, RE, & Jorgensen, EM (1999). The *Caenorhabditis elegans* unc-49 Locus Encodes Multiple Subunits of a Heteromultimeric GABA Receptor. *J Neurosci,* 19(13), 5348-5359.

Bamber, BA, Twyman, RE, & Jorgensen, EM (2003). Pharmacological characterization of the homomeric and heteromeric UNC-49 GABA receptors in *C. elegans. Br J Pharmacol* 138, 883-893.

Bamber, BA, Richmond, JE, Otto, JF, & Jorgensen, EM (2005). The composition of the GABA receptor at the *Caenorhabditis elegans* neuromuscular junction. *Br J Pharmacol* 144(4), 502-509.

Bartos M, Corradi J, Bouzat C (2009) Structural basis of activation of cys-loop receptors: the extracellular-transmembrane interface as a coupling region. *Mol Neurobiol*. 40(3):236-5

Beg AA, Jorgensen EM (2003) EXP-1 is an excitatory GABA-gated cation channel. *Nat Neurosci* 6(11):1145-52.

Best, RB, Zhu, X, Shim, J, Lopes, PEM, Mittal, J, Feig, M., and MacKerell Jr, AD (2012) Optimization of the additive CHARMM all-atom protein force field targeting improved sampling of the backbone phi, psi and side-chain chi1 and chi2 dihedral angles. *J Chem Theory and Comp*, 8: 3257-3273

Brejc K, van Dijk WJ, Klaassen RV, Schuurmans M, van Der Oost J, Smit AB, Sixma TK (2001) Crystal structure of an ACh-binding protein reveals the ligand-binding domain of nicotinic receptors. *Neuron* 411(6835):269-76.

del Olmo N, Bustamante J, del Rio RM, Solis JM (2000). Taurine activates GABA(A) but not GABA(B) receptors in rat hippocampal CA1 area. *Brain Res.* 864**:** 298-307

Hibbs RE, Gouaux E (2011) Principles of activation and permeation in an anion-selective Cys-loop receptor. *Nature* 474(7349):54-60.

Hosie AM, Aronstein K, Sattelle DB, ffrench-Constant RH (1997) Molecular biology of insect neuronal GABA receptors. *Trends Neurosci* 20(12):578-83

Hosie AM, Wilkins ME, da Silva HM, Smart TG (2006) Endogenous neurosteroids regulate GABA$_A$ receptors through two discrete transmembrane sites. *Nature* 444(7118):486-9

Humphrey W, Dalke A, Schulten K (1996) VMD: Visual molecular dynamics. *J Mol Graph* 14, 33–38. http://www.ks.uiuc.edu/Research/vmd/.

Irwin JJ, Sterling T, Mysinger MM, Bolstad ES, Coleman RG (2012). ZINC: a free tool to discover chemistry for biology. *J. Chem. Inf Model* 52**:** 1757-1768

Jones AK, Sattelle DB (2008) The cys-loop ligand-gated ion channel gene superfamily of the nematode, Caenorhabditis elegans. *Invert Neurosci*. 8(1):41-7

Kaji, MD, Kwaka, A, Callanan, MK, Nusrat, H, Desaulniers, JP, Forrester, SG (2015). A molecular characterization of the agonist binding site of a nematode cys-loop GABA receptor. *Br J Pharmacol* 172(15), 3737-47.

Kloda, JH, & Czajkowski, C (2007). Agonist-, Antagonist-, and Benzodiazepine-Induced Structural Changes in the α1Met[113]-Leu[132] Region of the GABA$_A$ Receptor. *Mol Pharm, 71(2),* 483-493.

Kusama T, Spivak CE, Whiting P, Dawson VL, Schaeffer JC, Uhl GR (1993). Pharmacology of GABA rho 1 and GABA alpha/beta receptors expressed in Xenopus oocytes and COS cells. *Br J Pharmacol* 109**:** 200-206

Laing R, Kikuchi T, Martinelli A, Tsai IJ, Beech RN, Redman E, Holroyd N, Bartley DJ, Beasley H, Britton C, Curran D, Devaney E, Gilabert A, Hunt M, Jackson F, Johnston SL, Kryukov I, Li K, Morrison AA, Reid AJ, Sargison N, Saunders GI, Wasmuth JD, Wolstenholme A, Berriman M, Gilleard JS, Cotton JA (2013) The genome and transcriptome of *Haemonchus contortus*, a key model parasite for drug and vaccine discovery. *Genome Biol* 28;14(8):R88.

Morris G, Huey R, Lindstrom W, Sanner M, Belew R, Goodsell D, Olson A (2009) AutoDock4 and AutoDockTools4: Automated Docking with Selective Receptor Flexibility. *J Compt Chem* 30:2785-2791

Newell JG, McDevitt RA, Czajkowski C (2004) Mutation of glutamate 155 of the GABA$_A$ receptor beta2 subunit produces a spontaneously open channel: a trigger for channel activation. *J Neurosci* 15;24(50):11226-35

Putrenko, I, Zakikhani, M, & Dent, JA (2005). A Family of Acetylcholine-gated Chloride Channel Subunits in *Caenorhabditis elegans. J Biol Chem* 280(8), 6392-6398

Sali A, Blundell TL (1993). Comparative protein modelling by satisfaction of spatial restraints. *J. Mol. Biol.* 234**:** 779-815

Sedelnikova, A, Smith, CD, Zakharkin, SO, Davis, D, Weiss, DS, Chang, Y (2005). Mapping the ρ1 GABA$_C$ Receptor Agonist Binding Pocket. *J Biol Chem* 280(2), 1535-1542.

Siddiqui, SZ, Brown, DDR, Rao, VTS, & Forrester, SG (2010). An UNC-49 GABA receptor subunit from the parasitic nematode *Haemonchus contortus* is associated with enhanced GABA sensitivity in nematode heteromeric channels. *J Neurochem* 113, 1113-1122.

Trott O, Olson AJ (2010). AutoDock Vina: improving the speed and accuracy of docking with a new scoring function, efficient optimization, and multithreading. *J. Comput. Chem.* 31**:** 455-461

Vanommeslaeghe K, Hatcher E, Acharya C, Kundu S, Zhong S, Shim J, Darian E, Guvench O., Lopes P, Vorobyov I, MacKerell AD Jr (2010) CHARMM General Force Field: A Force field for Drug-Like Molecules Compatible with the CHARMM All-Atom Additive Biological Force Field, *J. Comput. Chem.* 31, 671-690.

Vanommeslaeghe K, MacKerell Jr, AD (2012) Automation of the CHARMM General Force Field (CGenFF) I: bond perception and atom typing, *J. Chem. Inf. Model.* 52, 3144-3154.

Vanommeslaeghe K, Raman EP, MacKerell Jr, AD (2012) Automation of the CHARMM General Force Field (CGenFF) II: Assignment of bonded parameters and partial atomic charges, *J. Chem. Inf. Model.* 52, 3155-3168.

Wang J, Horenstein NA, Stokes C, Papke RL (2010) Tethered agonist analogs as site-specific probes for domains of the human α7 nicotinic acetylcholine receptor that differentially regulate activation and desensitization. *Mol Pharmacol* 78(6):1012-25

Wardell B, Marik PS, Piper D, Rutar T, Jorgensen EM, Bamber BA (2006) Residues in the first transmembrane domain of the *Caenorhabditis elegans* GABA(A) receptor confer sensitivity to the neurosteroid pregnenolone sulfate. *Br J Pharmacol* 148(2):162-72

Woodward RM, Polenzani L, Miledi R (1993). Characterization of bicuculline/baclofen-insensitive (rho-like) gamma-aminobutyric acid receptors expressed in Xenopus oocytes. II. Pharmacology of gamma-aminobutyric acidA and gamma-aminobutyric acidB receptor agonists and antagonists. *Mol. Pharmacol.* 43**:** 609-625

Yu W, He X, Vanommeslaeghe K, MacKerell Jr AD (2012) Extension of the CHARMM General Force Field to Sulfonyl-Containing Compounds and Its Utility in Biomolecular Simulations, *J. Comput. Chem.* 2012, 33, 2451-2468.

Figure Legends

Figure 1. Chemical Structures of GABA (gamma-aminobutyric acid), MTSET (2-(trimethylammonium) ethyl methanethiosulfonate), DAVA (5-aminovaleric acid), and Pregnenolone Sulfate (PS).

Figure 2. (A) Model of Hco-UNC-49B homodimer with a docked GABA molecule, highlighting Loop E residue positions (left) and the residues that face the binding pocket (right) based on the GluCl crystal structure (PDB 3RIF). **(B)** Sequence alignment of Hco-UNC-49B loop E residues with the loop E residues from other Cys-loop receptors (*Caenorhabditis elegans* UNC-49, *Brugia malayi* UNC-49, *Drosophila melanogaster* RDL, *Aplysia californica* GABA receptor alpha-like subunit, *Caenorhabditis elegans* EXP-1, *Ciona intestinalis* GABA alpha-6-like subunit, Human GABA$_A$, and Human GABA$_C$). Shaded area indicates positions not conserved between Hco-UNC-49B, Hsa-GABA$_A$ α1 and Hsa-GABA ρ1. Bar graph below alignment demonstrates the fold change in GABA EC$_{50}$ of Hco-UNC-49BC observed when each Hco-UNC-49B loop E amino acid was replaced with a cysteine via site-directed mutagenesis. Each bar represents an average fold change (n ≥ 6) ± SE Associated EC$_{50}$ values that were statistically different ($P>0.001$) from C224A are indicated by *. PBD File: Hco-UNC-49

Figure 3. (A) Representative electrophysiological tracings of Hco-UNC-49BC with mutated Hco-UNC-49B subunits H142C, C224A (cysteine-less mutant used as template for creation of other mutants), and S157C. **(B)** Dose-response curve of Hco-UNC-49B mutants showing differences in GABA sensitivity, with normalized currents. Each point represents a mean with bars of SE (n>6).

Figure 4. Impact of MTSET on current evoked from GABA activation of Hco-UNC-49BC receptors with mutated Hco-UNC49-B subunits. **(A)** Representative tracings of current elicited from GABA (EC_{20-50}) before and after MTSET application (1 mM, 1 min). **(B)** Percentage change in current from treatment of mutant Hco-UNC-49BC receptors with MTSET. Each bar indicates the mean $\pm$ SE (n>3). Black bars denote statistically significant difference from C224A ($P<0.001$).

Figure 5. Effect of Loop E H142C mutation in Hco-UNC-49B on Hco-UNC-49BC response to DAVA and Pregnenolone sulfate (PS). **(A)** DAVA dose-response curve comparing C224A and H142C mutant receptors. **(B)** Comparison of maximal current produced by GABA and DAVA in C224A and H142C mutant receptors. **(C)** PS dose-response curve comparing C224A and H142C mutant receptors. **(D)** Comparison of current inhibited by PS in the presence of GABA (EC_{50}) in C224A and H142C mutant receptors.

Figure 6: Molecular simulation snapshots of the Hco-UNC-49B homodimer with GABA docked. E185 is in loop B, S236 is in loop C, R87 is in loop D and H142, S144, R147, D149, Y155 and S157 are in loop E **A)** GABA interacting with nearby residues within the binding pocket. Grey dashed-lines represent the H-bonds. The orange coloured backbone and displayed loop E are part of the same subunit while the purple coloured regions belong to the other subunit of the dimer. **B)** Interaction between GABA, Y155, R147 and D149 and **C)** H142 interacting with S144. Loop E is presented in residue type colors. The positively charged residues are in blue, the negatively charged residues are in red, the polar residues are in green and non-polar residues are in white. **D)** Distance analysis between GABA and Y155 and S157 over the course of the simulation. The distances are calculated between the Oxygens of the OH group on the side chains of Y155 and S157 and Oxygens of GABA. Inset: Percent hydrogen bonding between residues and GABA. Residue

numbering for Hco-UNC-49B corresponds to the first methionine of the amino acid sequence. PBD File: Hco-UNC-49

Figure 7: MD analysis of the interactions between residues and GABA **A)** The minimum distance between the three Nitrogen atoms of R147 sidechain and the two Oxygen atoms of the GABA (black), and the Oxygen atom of the D149 side chain and the three Nitrogen atoms of the R147 side chain (red). The black line indicates an initial interaction between the R147 and the GABA molecule and separation after that, while the red line indicates an initial separation between the R147 and the D149 and interaction for the rest of the simulation. **B)** Minimum distances between the Oxygen and Nitrogen atoms in the backbone of the R147 and the Y155.

Figure 8: The minimum distance between the two Nitrogen atoms of H142 sidechain and the Oxygen atom of the S144 side chain.

PDB File: Hco-UNC-49B homodimer

List of Tables:

Table 1. Comparison of GABA EC_{50} and Hill slope values of Hco-UNC-49B mutants assembled as heteromeric Hco-UNC-49BC receptors. Fold change values indicate change in GABA EC_{50} of each mutant normalized to C224A mutant (cysteine-less mutant with wild type responses, used as template for creation of other Loop E mutants).

Mutant	EC_{50} ± S.E. (µM) (*Hill Coefficient* ± S.E.)	n	Fold Change
C224A	32.56 ± 2.29 (*1.37* ± 0.11)	7	1
H142C	2.70 ± 0.22 (*1.44* ± 0.07) *	7	0.1
N143C	199.69 ± 22.86 (*1.33* ± 0.11) *	7	6.1
S144C	133.76 ± 11.96 (*1.31* ± 0.07) *	7	4.1
F145C	383.53 ± 114.30 (*1.40* ± 0.04)	7	11.8
L146C	361.39 ± 42.59 (*1.30* ± 0.04) *	7	11.1
R147C	90.32 ± 6.54 (*1.82* ± 0.16) *	8	2.8
I148C	19.37 ± 2.62 (*1.53* ± 0.13)	8	0.6
D149C	39.79 ± 7.11 (*2.15* ± 0.27)	7	1.2
S150C	54.39 ± 6.95 (*1.78* ± 0.13)	7	1.7
D151C	36.11 ± 3.25 (*1.43* ± 0.08)	7	1.1
G152C	54.91 ± 5.01 (*1.48* ± 0.06)	7	1.7
T153C	122.21 ± 10.01 (*1.71* ± 0.08) *	6	3.8
V154C	104.05 ± 5.10 (*1.51* ± 0.14) *	7	3.2
Y155C	111.49 ± 10.68 (*1.64* ± 0.09) *	7	3.4
T156C	628.48 ± 50.61 (*1.71* ± 0.06) *	6	19.3
S157C	3683.50 ± 413.66 (*1.43* ± 0.09) *	8	113.1
Q158C	35.44 ± 6.63 (*1.44* ± 0.10)	7	1.1
R159C	3102.33 ± 130.43 (*1.53* ± 0.03) *	6	95.3

* Values significantly different from C224A ($P < 0.001$)

Table 2. EC_{50}, Hill Coefficient, and maximal responses of DAVA and GABA produced by mutant Hco-UNC-49BC receptors H142C and C224A.

Compound	H142C			C224A		
	EC_{50} ± S.E. (µM) (Hill Coefficient ± *S.E.)*	% Maximal GABA ± S.E.	n	EC_{50} ± S.E. (µM) (Hill Coefficient ± S.E.)	% Maximal GABA ± S.E.	n
DAVA	1353.2 ± 246.2 (1.15 ± 0.16)	86.5 ± 2.8*	7	2464 ± 107.2 (2.18 ± 0.1)	21.2 ± 2.7	5
GABA	2.7 ± 0.22* (1.44 ± 0.07)	100	7	32.56 ± 2.29 (1.37 ± 0.11)	100	7

*Values significantly different from C224A (P<0.001)
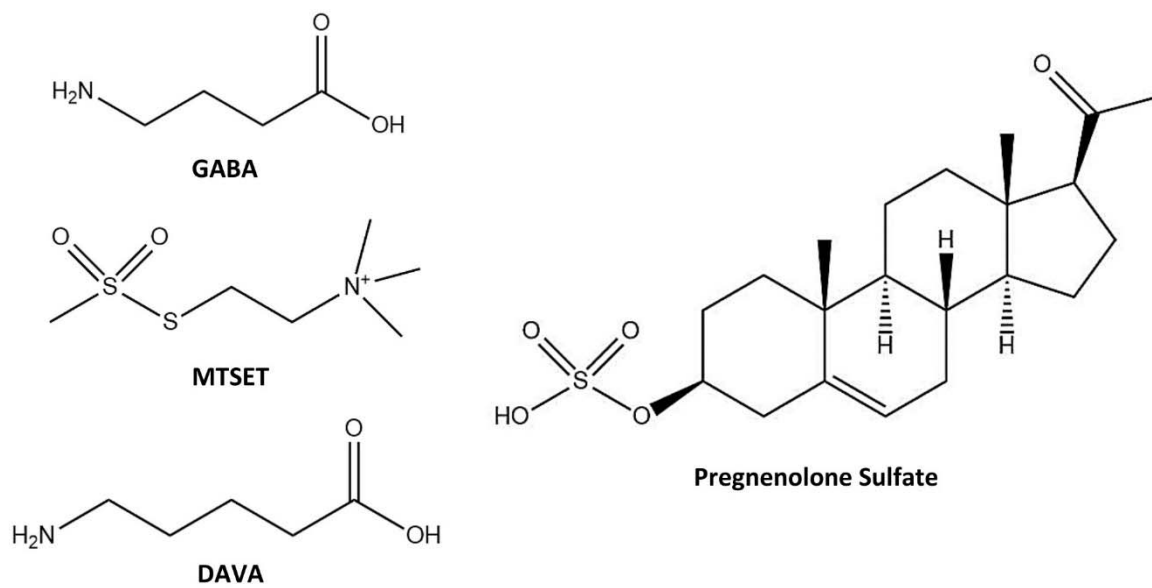
Figure 1
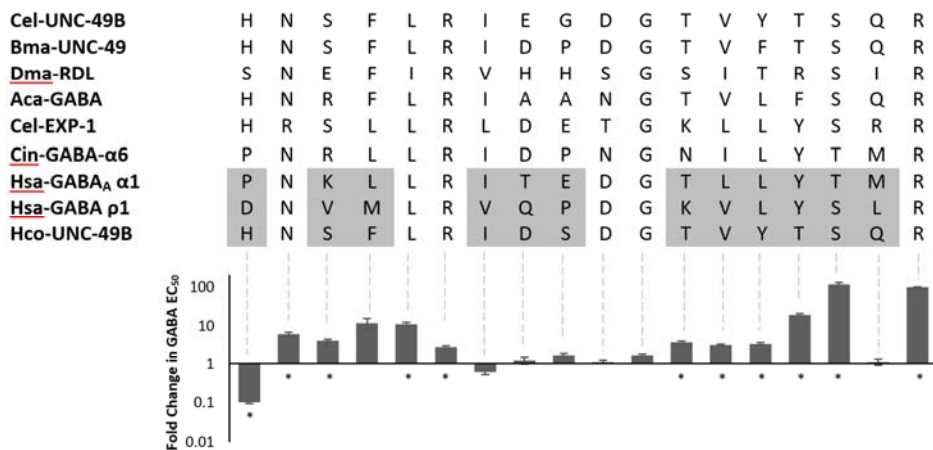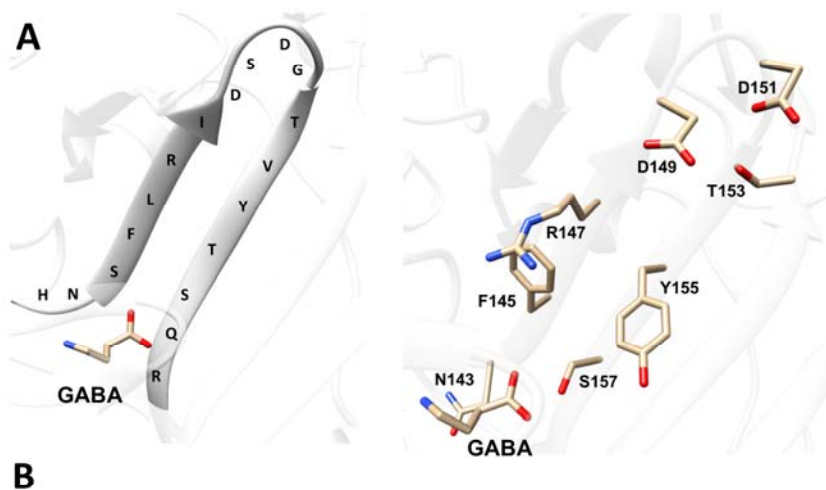
Figure 2
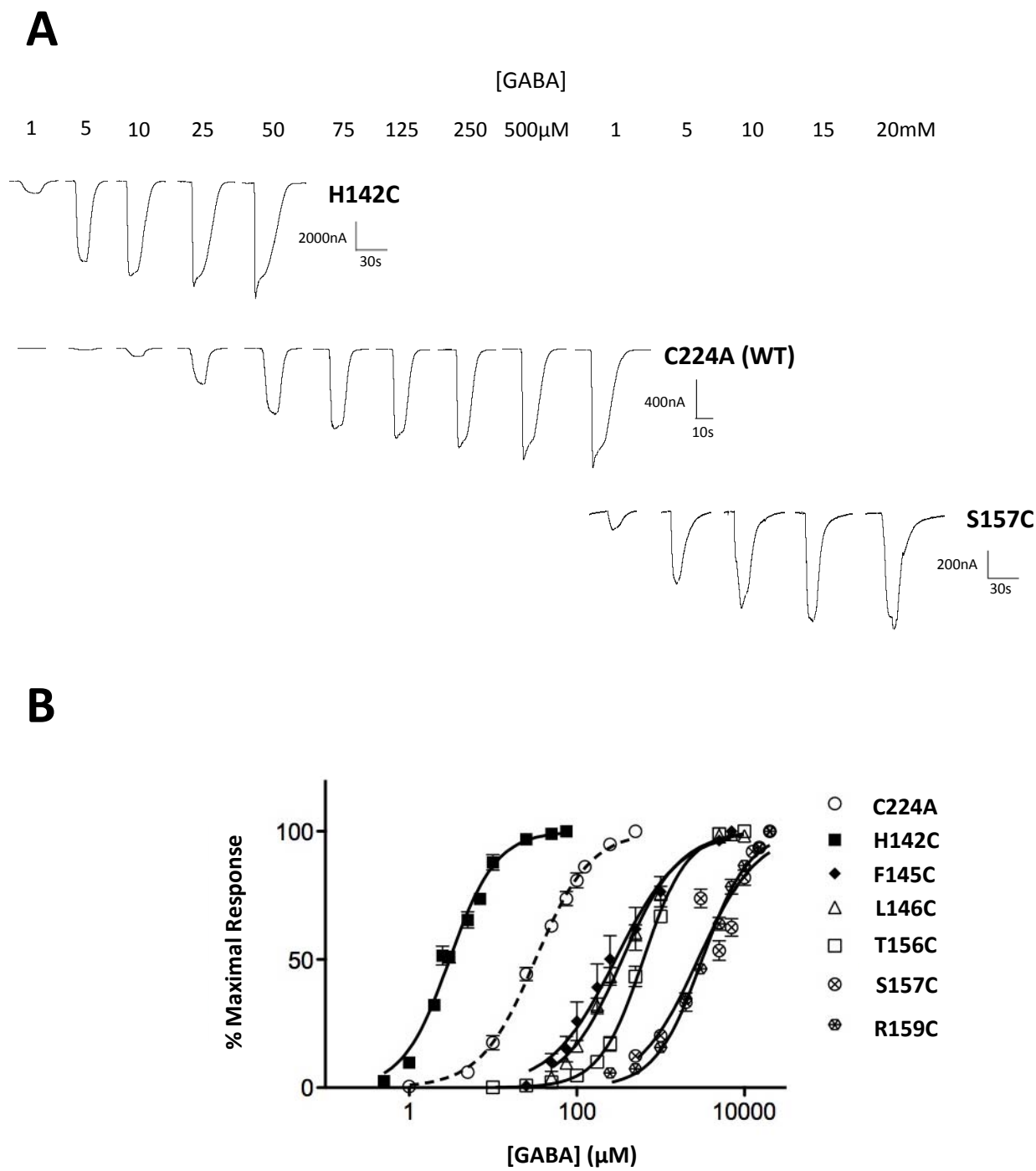
Figure 3
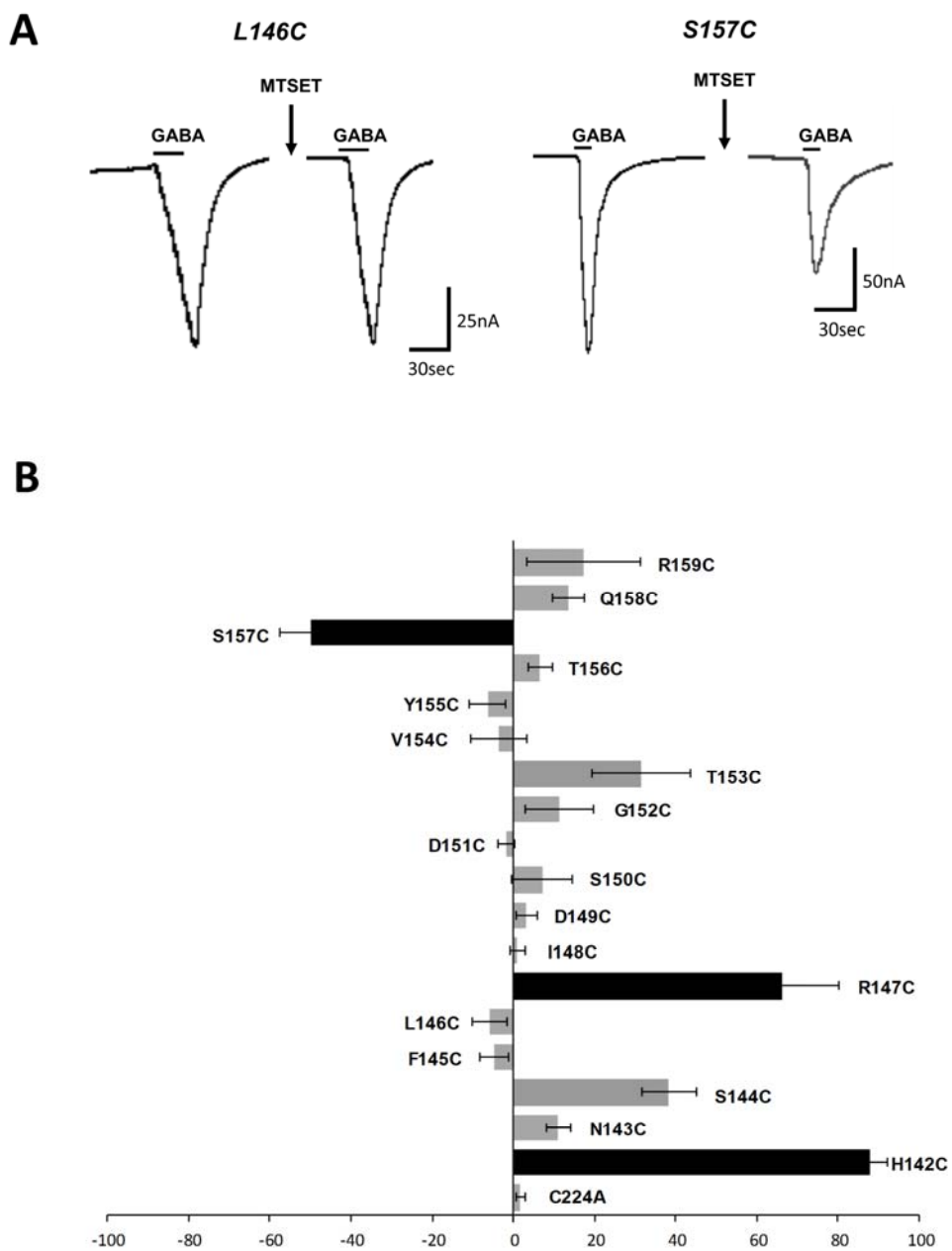
Figure 4
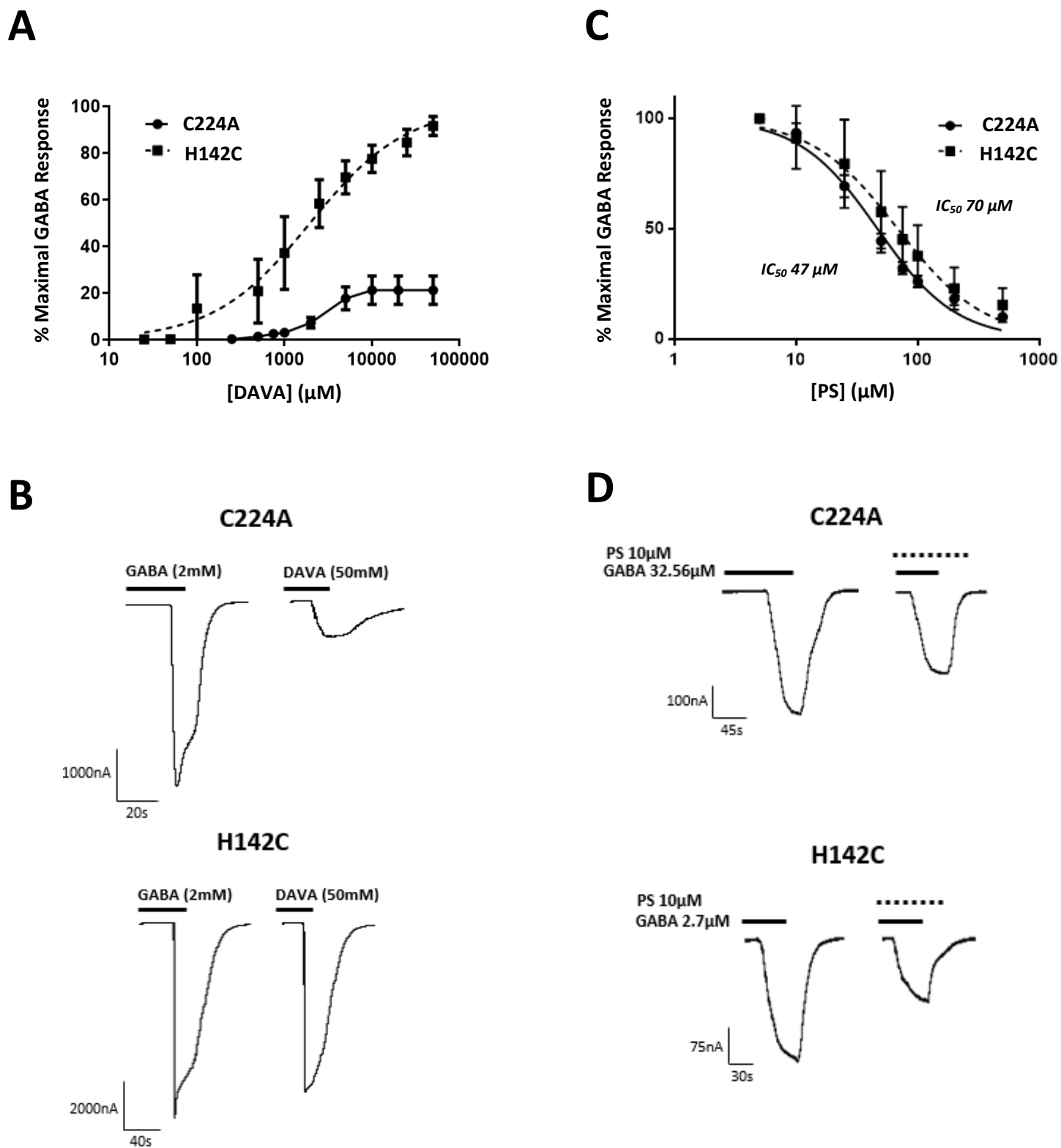
Figure 5
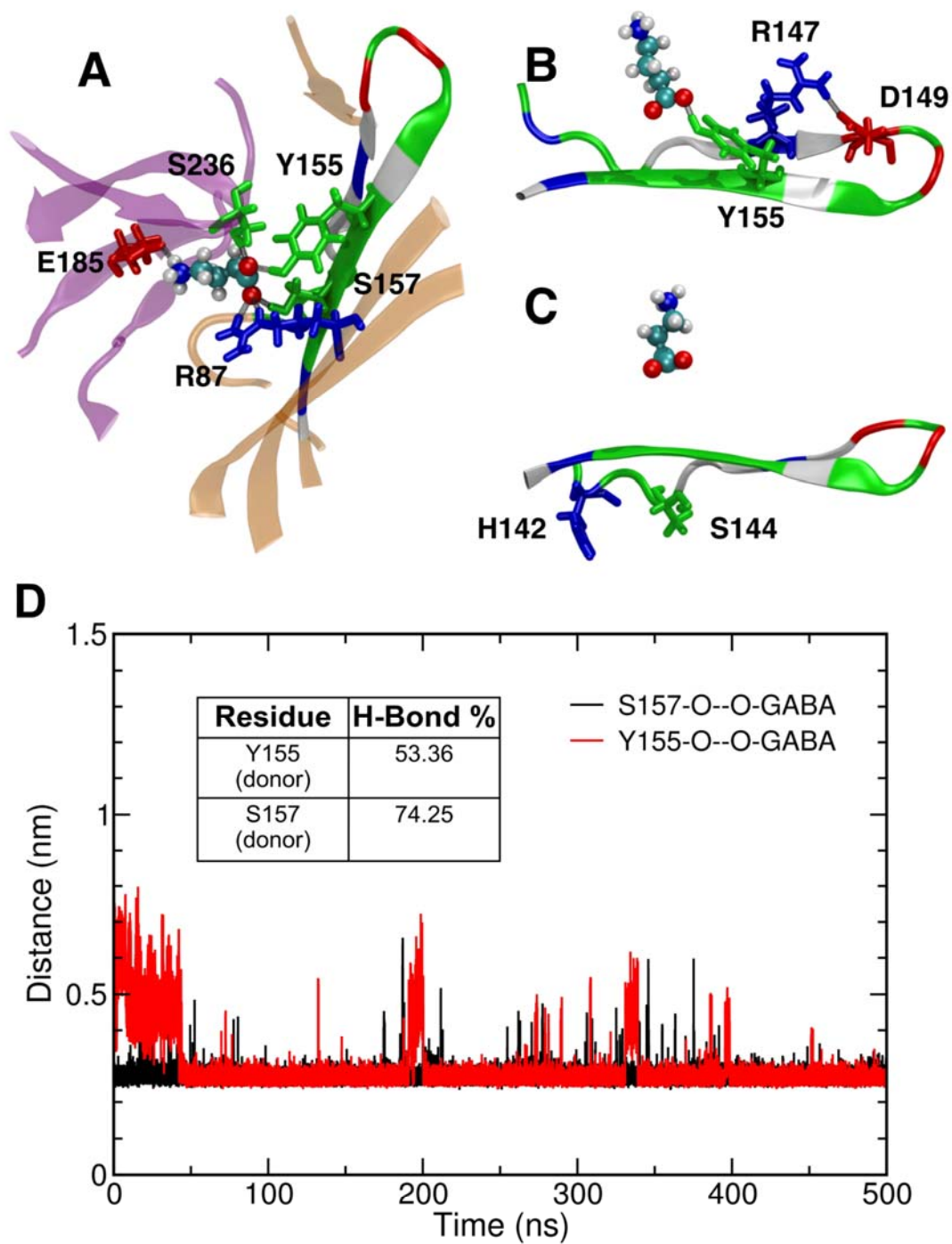
Figure 6

Figure 7

Figure 8

A molecular characterization of binding loop E in the nematode cys-loop GABA receptor

Ariel Kwaka, Mohammad H Khatami, Joshua Foster, Everett Cochrane, Sarah A Habibi, Hendrick W de Haan and Sean G. Forrester
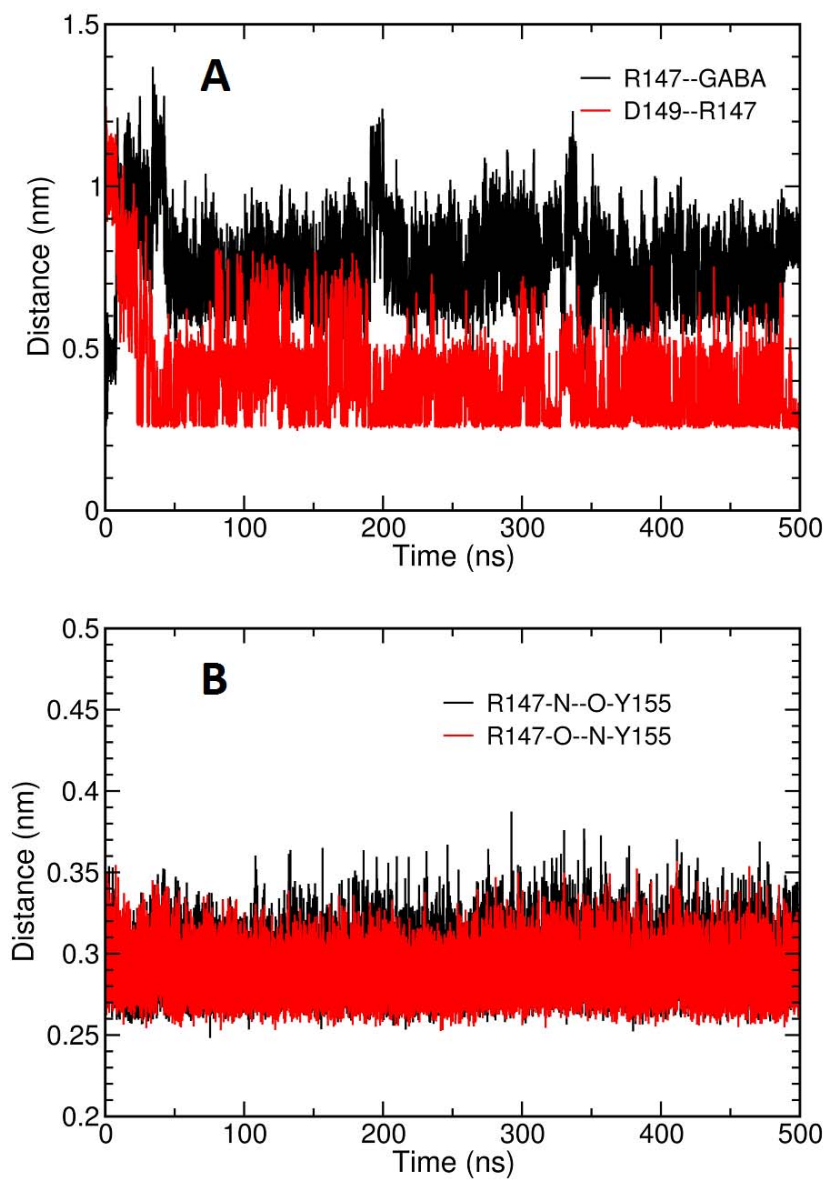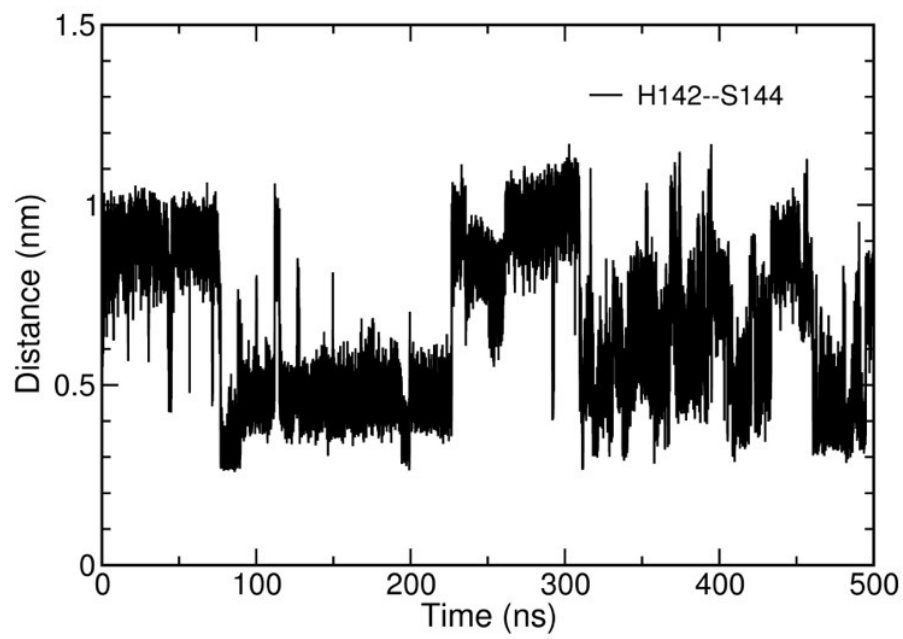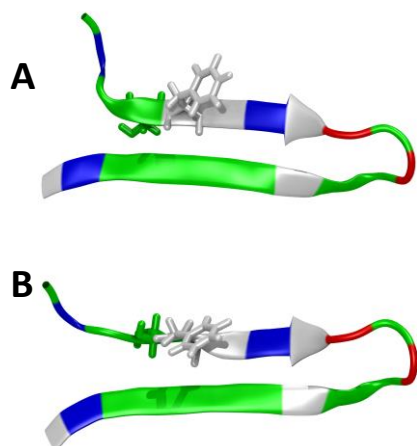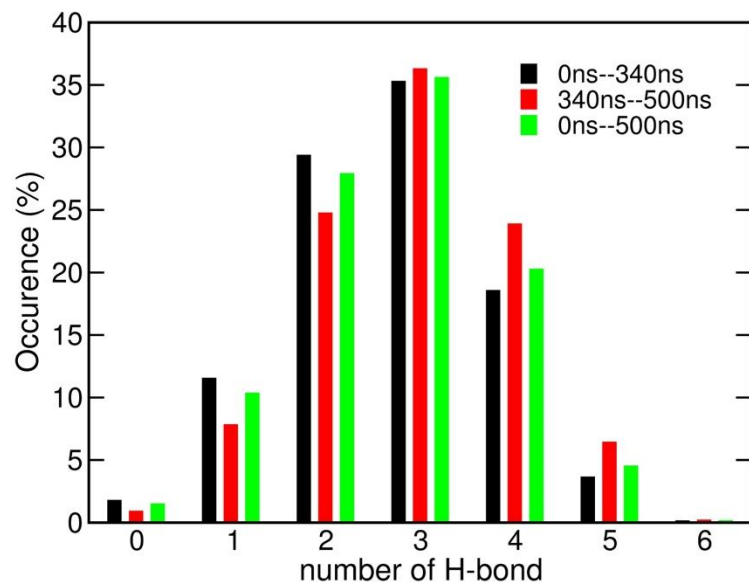
Supplemental Figure 1

Supplemental Figure 1: Snapshots of the loop E at t=1ns (A) and t=500ns (B), before and after the change in the structure of the loop (at t~300ns). Here, despite the changes in the structure of the loop, i.e., losing the secondary structure of the S144 and F145 residues, the general structure of the loop E remained in the β-sheet configuration. S144 is in green and F145 is in white. The β-sheet is colored by residue type. PBD File: Hco-UNC-49

A molecular characterization of binding loop E in the nematode cys-loop GABA receptor

Ariel Kwaka, Mohammad H Khatami, Joshua Foster, Everett Cochrane, Sarah A Habibi, Hendrick W de Haan and Sean G. Forrester

Supplemental Figure 2

Supplemental Figure 2: Histogram of number of H-bonds between the GABA molecules and the nearby residues for different time frames of the simulation. The default values (d<3.0Å and θ<20°) are used to determine the H-bonds. These results indicate that the GABA could form up to 6 H-bond with residues around it. PBD File: Hco-UNC-49

A molecular characterization of binding loop E in the nematode cys-loop GABA receptor

Ariel Kwaka, Mohammad H Khatami, Joshua Foster, Everett Cochrane, Sarah A Habibi, Hendrick W de Haan and Sean G. Forrester

Supplemental Table 1

Supplemental Table 1. Percentage of H-bond occurrence between GABA and residues on the loop E of the protein during different time frames of the simulation. Occurrences above 10% are reported.

Residue	H-bond percentage (%) 0ns–340ns	H-bond percentage (%) 340ns–500ns	H-bond percentage (%) 0ns–500ns
Y155 (donor)	48.22	64.30	53.36
S157 (donor)	72.23	78.55	74.25

A molecular characterization of binding loop E in the nematode cys-loop GABA receptor

Ariel Kwaka, Mohammad H Khatami, Joshua Foster, Everett Cochrane, Sarah A Habibi, Hendrick W de Haan and Sean G. Forrester

PDB File: Hco-UNC-49B homodimer